

Climatology and trends of Aerosol Optical Properties and Direct Radiative Effect of main aerosol types based on MERRA-2 reanalysis data

Korras-Carraca M.B.^{1,2*}, Gkikas A.³, Matsoukas C.² and Hatzianastassiou N.¹

¹ Laboratory of Meteorology and Climatology, Department of Physics, University of Ioannina, 45110 Ioannina, Greece

² Department of Environment, University of the Aegean, 81100 Mytilene, Greece

³ Institute for Astronomy, Astrophysics Space Applications and Remote Sensing, National Observatory of Athens, 15236 Athens, Greece

*corresponding author e-mail: koras@env.aegean.gr

Abstract: Monitoring aerosol optical properties and their long-term fluctuations can improve the assessment of the induced Direct Radiative Effects (DREs) and the subsequent climatic impacts. A suitable database for such an investigation has been made available by the Modern-Era Retrospective analysis for Research and Applications, Version 2 (MERRA-2). In the present study, we investigate the spatio-temporal variation of the aerosol optical properties and clear-sky DREs of the main aerosol species (desert dust, sea salt, sulfate, organic and black carbon), and the total aerosol. To realize, MERRA-2 reanalysis products, at $0.5^\circ \times 0.625^\circ$ resolution, are used as inputs to the FORTH deterministic spectral radiation transfer model (RTM). Clear-sky shortwave (SW) DREs have been calculated at global scale and on a monthly basis, over the period 1980–2019 (40 years), at the surface, within the atmosphere and at the top-of-the-atmosphere. According to our results, during the study period, the DREs exhibited changes in magnitude. More specifically, a strong increase of aerosol-induced atmospheric warming was observed which, in combination with an increase of surface cooling effect resulted in a slight decrease of the clear-sky TOA cooling from -5.48 Wm^{-2} during the 1980s to -5.23 Wm^{-2} during the 2010s.

1 Introduction

Aerosol particles, among other atmospheric constituents, through their direct and indirect interaction with radiation, exert a perturbation of the Earth-Atmosphere system energy budget, thus playing a key role in the current and future climate. Originating from natural and anthropogenic sources worldwide, their microphysical and optical radiative properties are strongly dependent on particles' composition and they are highly variable both in space and time. Moreover, the vertical structure of aerosol layers as well as the underlying surface properties impose a further complexity in the assessment of the relevant radiative effects. In order to quantify the aerosol DREs, at global and regional scale, an accurate speciation of aerosol types is required, as well as an optimum characterization of their key optical properties, namely the aerosol optical depth (AOD), single scattering albedo (SSA) and asymmetry parameter (g), taking into account their 3-D distribution. A comprehensive climatological analysis of aerosol radiative effects aiming at reducing the current uncertainty levels reported by IPCC, 2013 requires the use of long-term global databases of aerosol optical properties per particle type and the estimation of their respective radiative effect, as well as their contribution to the total perturbation of radiation at long-term (i.e. decadal) scales. Such a long-term aerosol database has been made available recently through Modern-Era Retrospective analysis for Research and Applications, Version 2 (MERRA-2, Gelaro et al. 2017). In this study, 40 years (1980–2019) of MERRA-2 reanalysis data are used as input to a radiative transfer model in order to investigate the spatio-temporal variation of the clear-sky direct radiative effects (DREs) per aerosol type as well as for the total aerosol.

2 Data and Methodology

The aerosol DREs are computed using the deterministic spectral radiation transfer model FORTH (Hatzianastassiou et al., 2007), developed from a radiative-convective model (Vardavas and Carver, 1984). The model computations are performed on a monthly basis and $0.5^\circ \times 0.625^\circ$ horizontal resolution (the original MERRA-2 resolution), for 118 wavelengths ranging from $0.20 \mu\text{m}$ to $1 \mu\text{m}$ and for 10 spectral intervals between 1 and $10 \mu\text{m}$. For each wavelength and spectral interval, the monochromatic radiative flux transfer equations are solved for an absorbing/multiple-scattering atmosphere using the Delta-Eddington method.

In order to calculate the aerosol DREs, the FORTH RTM requires their vertically and spectrally resolved optical properties (Aerosol Optical Depth or AOD, Single Scattering Albedo or SSA, and asymmetry parameter or g). Such data are not provided directly by MERRA-2 reanalysis. Therefore, we computed them based on MERRA-2 vertically resolved (72 layers), 3-hourly instantaneous aerosol mixing ratios and relative humidity data, along with look-up tables providing

spectrally resolved (25 wavelengths) scattering and absorption efficiencies per aerosol type, size bin and relative humidity. Apart from aerosols, all remaining RTM required input data (meteorological fields, ozone and surface albedo) are also taken from MERRA-2. The RTM input data are averaged during each month of the 40-year period 1980-2019. The aerosol DREs are computed at the Earth's surface, within the atmosphere and at the Top of the Atmosphere (TOA) as $DRE_x = F_{aer_x} - F_{no_aer_x}$, where x corresponds to the particle type (sulfate, sea-salt, dust, organic carbon, black carbon and total) while F_{aer} and $F_{no_aer_x}$ are the net downward (downward minus upward) radiative fluxes obtained running the RTM with all aerosol types and without considering a particular aerosol type x, respectively. In the case of $x=total$, $F_{no_aer_x}$ corresponds to the model run without aerosols.

3 Results

The spatial distribution of the annual mean values of columnar MERRA-2 total AOD at 550 nm, averaged over the 40-year period 1980–2019, is shown in Fig. 1a. A significant spatial variability of the AOD is evident, with higher aerosol load above land regions, especially in the Northern Hemisphere. More specifically, very high aerosol load (AOD up to 0.68) is observed in the densely populated region of east Asia and especially, China. In this region, according to MERRA-2 (results not shown here) the aerosol load is dominated by sulfate particles, but also by significant loads of carbonaceous (organic and black carbon) particles. Relatively high AOD (0.3-0.4), associated with anthropogenic sources, is also found above other regions, such as the Indian subcontinent and especially the Indo-Gangetic Plain. Over arid and semi-arid regions of the planet, the aerosol load is dominated by dust and the AOD values reach up to 0.70 (above the Sahara desert). High aerosol loads (up to 0.2-0.4, locally) are also evident over regions with frequent seasonal biomass burning (such as the Southern Africa and America), and therefore strong presence of carbonaceous particles. On the other hand, low AOD is observed above most oceanic regions, except in cases where continental particles are advected. Such a characteristic case is the Saharan dust outflow to the tropical and subtropical North Atlantic Ocean and the export of biomass burning to the Gulf of Guinea or the southeastern Atlantic Ocean (off the coasts of Gabon, Kongo, Angola).

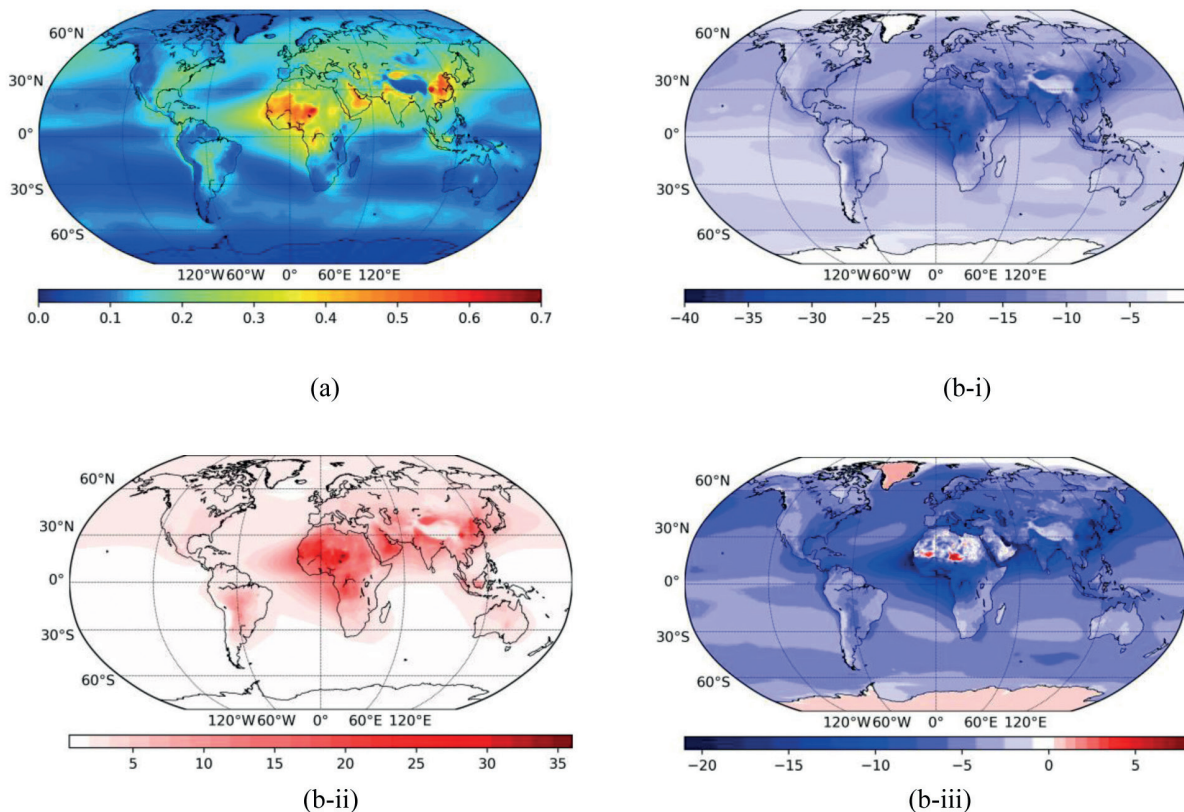


Fig. 1. Mean annual (1980-2019) global distribution of: (a) MERRA-2 Optical Depth for the total aerosol load at the wavelength of 550 nm and (b) total aerosol Direct Radiative Effects (Wm^{-2}): (i) at the Earth's surface, (ii) within the Atmosphere and (iii) at the Top Of the Atmosphere.

The mean annual geographical distribution of the clear-sky aerosol effects on the net shortwave flux at the Earth's surface (hereafter $DRE_{surfnet}$), within the atmosphere (DRE_{atm}) and at TOA (DRE_{TOA}), averaged over the entire study period, is presented in Fig. 1b.

At the Earth's surface (Fig. 1b-i), aerosols cause a cooling effect (negative $DRE_{surfnet}$). This cooling arises from the reduction of the downwelling solar radiation due to scattering and absorption by aerosol particles. The surface cooling is more pronounced (up to 40 Wm^{-2}) over regions with high aerosol load, of both natural (such as desert dust) and anthropogenic (such as sulfate) origin. More specifically the strongest cooling is observed over East Asia, Central and North Africa, the Arabian Peninsula, South America and the Indian Subcontinent, as well as above neighboring oceanic regions where aerosols are transported from the former source areas.

The aerosol effect within the atmosphere is presented in Fig. 1b-ii. It is evident that aerosols cause a heating of the atmosphere (by increasing the atmospheric absorption). This heating effect is stronger in regions with high AOD and relatively absorbing aerosols, such as desert dust and carbonaceous particles. Although DRE_{atm} has an opposite sign to that of $DRE_{surfnet}$, their geographic distributions are similar and the magnitudes comparable. The atmospheric heating is especially pronounced above Central and North Africa with the DRE_{atm} reaching locally 36 Wm^{-2} over the Southern Saharan Desert.

The aerosol DRE at TOA (Fig. 1b-iii) is the sum of the DREs at the Earth's surface and within the atmosphere, which tend to counterbalance each other. The values of DRE_{TOA} range from -21 to 8 Wm^{-2} . Negative values indicate decreasing net incoming solar radiation (i.e. planetary cooling due to increased backscattered solar radiation to space), while positive values indicate a planetary warming. In most parts of the globe the aerosol surface cooling is more pronounced than the warming effect within the atmosphere, therefore the overall DRE at TOA is of negative sign. The cooling effect is more pronounced in East Asia, Central Africa, Sahel and Sub-Sahel regions. A very strong planetary cooling is also observed above oceanic regions where continental aerosols are advected (especially the tropical Atlantic Ocean and the Northern Indian Ocean). On the other hand, above regions characterized by high surface albedo (such as deserts and ice- and snow-covered polar regions) DRE_{TOA} is either small or of positive sign (i.e. planetary warming effect). The TOA warming effect is more pronounced in parts of the Sahara desert (up to 8 Wm^{-2} in Bodélé) due to the combination of the presence of relatively absorbing desert dust aerosols and the underlying highly reflective surface. The warming effect (up to 2 Wm^{-2}) in the polar regions is of particular interest because of their climatic sensitivity.

The globally and hemispherically averaged values of the aerosol DREs, as well as the DREs averaged over global land and ocean areas, are computed for each decade of the study period (1980-1989, 1990-1999, 2000-2009 and 2010-2019), in order to provide some insight about their temporal variability and are presented in Fig. 2. We provide the DREs corresponding to the total aerosol load (1st row) as well as for each aerosol particle type separately (i.e. sulfate, dust, sea salt, organic carbon and black carbon; 2nd to 6th row in Fig. 2).

According to Fig. 2, large differences between the DREs of different aerosols are evident. On global level, the strongest surface cooling is caused by desert dust and sulfate particles. The atmospheric warming is proportional to the particle absorptivity and therefore the main contributors of this effect are black carbon particles followed by dust. The heating effect of the almost purely scattering sea-salt and sulfate is small, as expected. At TOA, the strongest cooling is caused by sulfate and sea salt particles. The DREs of all particles at TOA are negative (i.e. cooling effect), with the exception of black carbon aerosols, which cause a heating effect. The aerosol DREs exhibit differences in their magnitude between land and oceans as well as between the two hemispheres. Generally, the aerosol effects are larger over land than over ocean and over the Northern Hemisphere compared to the Southern (especially for dust). These differences are more pronounced for the DRE_{atm} and they are related to the presence of stronger and more absorbing aerosols over the Northern Hemisphere and global land areas.

The temporal variation of the aerosol DREs is of particular interest due to the subsequent climatic consequences. One of the most characteristic features of the temporal variation is the smaller sulfate DREs during the 2000s and 2010s (mean global values at TOA -1.21 and -1.11 Wm^{-2}) compared to 1980s and 1990s (DRE_{TOA} -1.96 and -2.47 Wm^{-2} , respectively). This decrease is caused by a large reduction in sulfur emissions mainly in Europe and North America and the subsequent decrease of sulfate AOD (results not shown here). The sulfate DREs are also strongly affected by the increase of sulfate load within the atmosphere due to Mt. Pinatubo eruption in 1991, resulting in a large cooling effect at TOA during the 1990s.

Overall, between 1980s and 2010s, the total aerosol load DREs at the Earth's surface and within the atmosphere increased in absolute values. More specifically, the surface cooling slightly increased from -8.44 to -9.17 Wm^{-2} , since the decreased sulfate $DRE_{surfnet}$ was compensated by an increased cooling from dust, organic and black carbon particles. The increase of the aerosol-induced atmospheric warming effect was larger (from 2.97 Wm^{-2} during the 1980s to 3.95 Wm^{-2} during the 2010s) and is due to increasing black carbon DRE_{atm} . Overall, these changes resulted in a slight decrease of the TOA cooling effect from -5.48 to -5.23 Wm^{-2} on the global average scale.

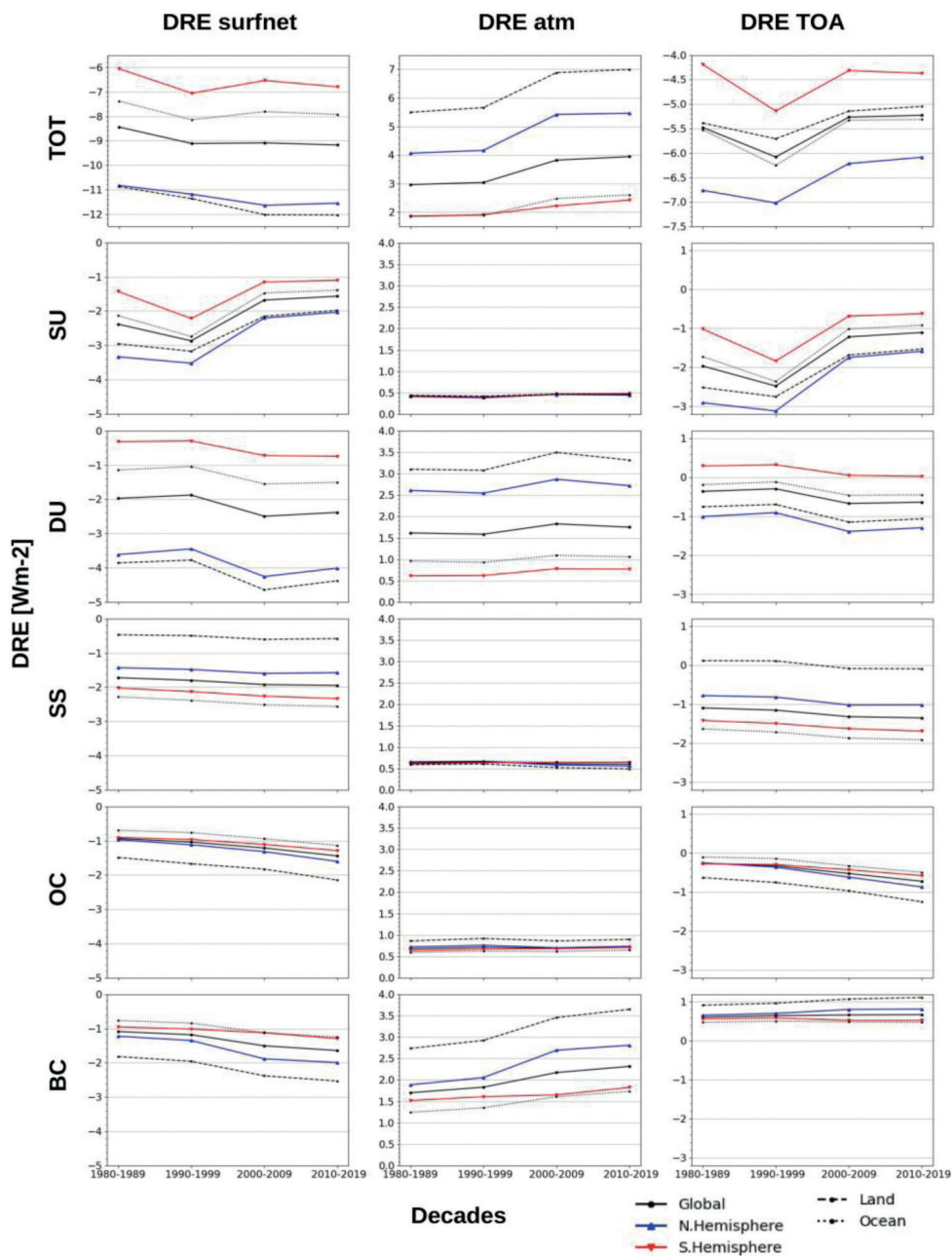


Fig. 2. Long-term (decadal) averaged aerosol DRE (in Wm^{-2}) at the Earth’s surface (1st column), within the Atmosphere (2st column) and at the Top Of the Atmosphere (3rd column), over the globe (black line), the Northern and Southern Hemispheres (blue and red lines), land (black dashed line) and ocean (black dotted line). The results are provided for the total aerosol load (fist raw) and for sulfate (SU), dust (DU), sea salt (SS), organic(OC) and black carbon (BC) particles (2nd to 6th row, respectively).

4 Conclusions

In this study, we investigated the spatio-temporal variation of the aerosol optical properties and directradiative effects (DREs) under clear-sky conditions, during 1980-2019, on a global scale, using MERRA-2 reanalysis data and the FORTH deterministic spectral radiative transfer model. We found high AOD values (up to 0.70) above regions where the aerosol load consisted of both natural and anthropogenic particles, such as East Asia (high loads of sulfate particles) and North Africa (mainly desert dust and carbonaceous particles). Our model results revealed a surface cooling up to $40 Wm^{-2}$ and an atmospheric warming up to $36 Wm^{-2}$ during 1980-2019, in regions with high aerosol load, located especially in continental parts of the Northern Hemisphere. The surface cooling and atmospheric warming effects resulted in a planetary cooling effect at TOA above most parts of the globe, which was found to be stronger (up to $21 Wm^{-2}$) over ocean regions undergoing advection of particles of continental origin (such as the tropical North Atlantic Ocean). An

aerosol planetary warming effect was found above regions characterized by large surface albedo, with the DRE_{TOA} reaching 8 Wm^{-2} above the Sahara desert and 2 Wm^{-2} above Greenland and Antarctica. On global level the DRE_{TOA} was -5.23 Wm^{-2} during the 2010s (2010-2019); slightly lower than during the 1980s (-5.48 Wm^{-2}). However, this small decrease resulted from a strong increase of the DRE_{atm} (from 2.97 Wm^{-2} to 3.95 Wm^{-2}) and an increase of surface cooling (-8.44 to -9.17 Wm^{-2}). These changes are mainly related to the change of the aerosol load composition and more specifically to the sharp decrease of sulfuric emissions in Europe and North America and the increase of dust, organic and black carbon AOD. The increase of black carbon particles is of particular interest because, despite their relatively small optical depth, they cause a substantial TOA heating, which during the last decade of our study period reached 0.67 Wm^{-2} on a mean global level. This heating effect is partially compensating the global cooling effect of aerosols at TOA. The aerosol induced cooling of the Earth's surface and warming of its atmosphere can have consequences for the dynamics of the Earth-atmosphere system, which deserves to be investigated.

Acknowledgments This research (grant number 1052) is implemented through the Operational Program “Human Resources Development, Education and Lifelong Learning” and is co-financed by the European Union (European Social Fund) and Greek national funds. The authors sincerely thank Dr Arlindo Da Silva at the Global Modeling and Assimilation Office (GMAO), NASA/Goddard Space Flight Center for his help during the processing of MERRA-2 data.

References

- Boucher, O., Randall, D., Artaxo, P., Bretherton, C., Feingold, G., Forster, P., Kerminen, V.-M., Kondo, Y., Liao, H., Lohmann, U., Rasch, P., Satheesh, S. K., Sherwood, S., Stevens, B., Zhang, X. Y. (2013) Clouds and Aerosols, in: *Climate Change 2013: The Physical Science Basis, Contribution of Working Group I to the Fifth Assessment Report of the Intergovernmental Panel on Climate Change*, Stocker, T. F., Qin, D., Plattner, G.-K., Tignor, M., Allen, S. K., Boschung, J., Nauels, A., Xia, Y., Bex, V. and Midgley, P. M., Eds. Cambridge University Press: Cambridge, UK and New York, NY, USA, 2013 pp. 571–658
- Gelaro, R., McCarty, W., Suárez, M.J., Todling, R., Molod, A., Takacs, L., Randles, C.A., Darmenov, A., Bosilovich, M.G., Reichle, R., Wargan, K., Coy, L., Cullather, R., Draper, C., Akella, S., Buchard, V., Conaty, A., da Silva, A., Gu, W., Kim, G. K., Koster, R., Lucchesi, R., Merkova, D., Nielsen, J.E., Partyka, G., Pawson, S., Putman, W., Rienecker, M., Schubert, S.D., Sienkiewicz, M., Zhao, B. (2017) The modern-era retrospective analysis for research and applications, version 2 (MERRA-2). *Journal of Climate*, 30(14), 5419-5454. doi:10.1175/JCLI-D-16-0758.1
- Hatzianastassiou, N., Matsoukas, C., Drakakis, E., Stackhouse Jr., P., Koepke, P., Fotiadi, A., Pavlakis, K., Vardavas, I. (2007) The direct effect of aerosols on solar radiation based on satellite observations, reanalysis datasets, and spectral aerosol optical properties from Global Aerosol Data Set (GADS). *Atmos. Chem. Phys.* 300 7, 2585–2599. doi: 10.5194/acp-7-2585-2007
- Vardavas, I. and Carver, J. H. (1984) Solar and terrestrial parameterizations for radiative convective models, *Planet. Space Sci.*, 32, 1307–1325. doi: 10.1016/0032-0633(84)90074-6